Int. J. Electron. Commun. (AEÜ) 159 (2023) 154464

Contents lists available at ScienceDirect

International Journal of Electronics and Communications

journal homepage: www.elsevier.com/locate/aeue

Regular paper

Design technique to mitigate unwanted coupling in densely packed radiating elements of an antenna array for electronic devices and wireless communication systems operating in the millimeter-wave band

Ayman A. Althuwayb [a,*], Mohammad Alibakhshikenari [b,*], Bal S. Virdee [c], Harry Benetatos [c], Nasr Rashid [a], Khaled Kaaniche [a], Ahmed Ben Atitallah [a], Osama I. Elhamrawy [a]

[a] Department of Electrical Engineering, College of Engineering, Jouf University, Sakaka, Aljouf 72388, Saudi Arabia
[b] Department of Signal Theory and Communications, Universidad Carlos III de Madrid, 28911 Leganés, Madrid, Spain
[c] London Metropolitan University, Center for Communications Technology, School of Computing & Digital Media, London N7 8DB, UK

A R T I C L E I N F O

Keywords:
Antenna array
Beam steering
Metamaterials
Millimeter-wave devices
5G & 6G
Automotive radar

A B S T R A C T

A feasibility study of an innovative design is presented of a metamaterial inspired antenna array for millimeter-wave band applications where non-mechanical beam-steering is required such as in 5G and 6G communications, automotive and radar systems. In communication systems beam-steering antennas can significantly improve signal-to-noise ratio, spatial directivity, and the efficiency of data transmission. However, in tightly packed arrays the effects of mutual coupling between the radiating elements can severely limit the array's performance. The proposed antenna array consists of a 3 × 3 matrix of patch radiators that are tightly packed and interconnected to each other. Rows of radiators are demarcated by a horizontal microstrip transmission-line whose ends are short-circuited to the ground-plane. This technique reduces unwanted surface waves that contribute to undesired coupling. Embedded in the square patch radiators is a rhombus shaped slot that increases the effective aperture of the antenna with no impact on the antenna's size. As the antenna is excited via a single feedline the edge-to-edge spacing between the radiators and the interconnected feedlines are made such that there is phase coherency at the radiating elements. Measured results show that the effectiveness of the proposed array in simultaneously improving its impedance bandwidth and radiation characteristics. The measured peak gain and radiation efficiency are 13.6 dBi and 89.54 %, respectively.

1. Introduction

The International Telecommunication Union (ITU) has allocated millimeter-wave spectrum across 26 GHz and 40 GHz bands for use of mobile technology, including 5G and beyond systems [1]. This decision will pave the way for governments and regulators around the world to make these bands available for ultra-fast services. In fact, millimeter wave boosted networks will enable the delivery of multi-gigabit speeds, capacity, and exceptionally mobile broadband speeds in suburban areas and rural communities. Because millimeter-waves cannot penetrate buildings, they can only be used for short distance applications in densely populated areas where data congestion might be a problem, e.g., in sports stadiums, malls, and convention centers.

Beam-steering antenna arrays are fundamental components of massive multiple input multiple output (MIMO) systems of 5G that make possible expansion in system capacity and extension in coverage. In fact, antenna arrays are used in other systems including automotive and radars. This technology is essential to increase the resiliency (signal-to-noise ratio) of a transmitted signal and the channel capacity, without increasing spectrum usage, a common frequency can be steered simultaneously in multiple directions [2–8].

The continuing demand to reduce the size of the wireless systems is a challenging requirement for antenna designers. This is because the antenna size is related to the operating wavelength. In the case of antenna arrays, this entails reducing the spacing between adjacent radiating elements [910]. The consequence of tightly packing antennas in an array

* Corresponding authors.
E-mail addresses: aaalthuwayb@ju.edu.sa (A.A. Althuwayb), mohammad.alibakhshikenari@uc3m.es (M. Alibakhshikenari), b.virdee@londonmet.ac.uk (B.S. Virdee), h.benetatos@londonmet.ac.uk (H. Benetatos), nasrrashid@ju.edu.sa (N. Rashid), kkaaniche@ju.edu.sa (K. Kaaniche), abenatitallah@ju.edu.sa (A. Ben Atitallah), oiibrahim@ju.edu.sa (O.I. Elhamrawy).

https://doi.org/10.1016/j.aeue.2022.154464
Received 24 August 2022; Accepted 5 November 2022
Available online 17 November 2022

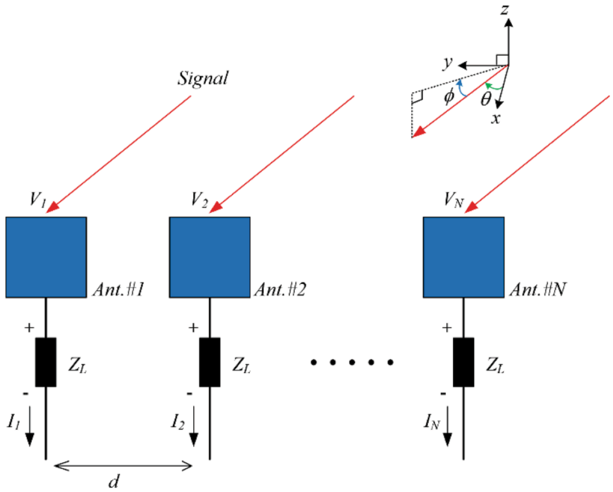

Fig. 1. Linear antenna array model.

will inevitably increase the electromagnetic coupling between the radiators. This will adversely affect the antenna parameters such as terminal impedances, impedance bandwidth and therefore the array's performance in terms of radiation characteristics, output signal-to-interference noise ratio, and radar cross section. In the case of radars this can undermine the system's steady state and transient response, the resolution, interference rejection, and direction-of-arrival estimation [11].

Therefore, the challenge is to shrink the footprint of antenna arrays and simultaneously suppress the mutual coupling between the neighboring radiation elements [12]. Various methods have been investigated and reported recently in literature in minimizing unwanted coupling in antenna arrays[13]. Some of these methods include using (i) frequency selective surfaces [14], hybrid feeding [15], metasurface slabs [16], electromagnetic bandgap (EBG) [17], parasitic structures [18], and metamaterials [19–21]. These prior approaches are challenging to implement especially in relatively small antenna array structures and require multiple excitation ports.

In this paper an innovative technique is proposed for the first time that can effectively mitigate mutual coupling between radiating elements in an antenna array. The proposed technique excludes incorporation of separate decoupling structures within the arrays. The proposed technique is applied to a millimeter-wave antenna array of small footprint that is constructed from 3 × 3 matrix of interconnected square patches. The patches are loaded with a rhombus shaped slot, and the rows of radiating patches are partitioned from each other with horizontal short circuited microstrip transmission-line. The resulting metamaterial inspired structure effectively mitigates mutual coupling between the radiators. The array only requires excitation using a single feed port. In the structure the gap between the radiator elements and lengths of the interconnected feedlines is made such that there is phase coherency at the radiators. The measured results confirm that compared to other recent mutual coupling mitigation techniques the proposed design approach provide improvement in the array's performance in terms of gain (13.6 dBi) and radiation efficiency (89.54 %) across 33 GHz to 37 GHz. In addition, the design and manufacture of the antenna is straightforward.

2. Modelling mutual coupling effect

Consider an antenna array comprising a single row of radiating elements, as illustrated in Fig. 1, where N radiating elements are uniformly spaced by a distance d, and an incoming signal of wavelength λ arrives at an azimuth and elevation angles of θ and ϕ, respectively. In this theoretical model, it is assumed that individual radiating elements in the array is a point source. In-reality this is not the case as each element will have a physical presence, and the mutual coupling effect is therefore inevitable. Mutual coupling will modify the current distribution of each radiating element thereby adversely impacting on the array's parameters, i.e., realized gain, efficiency, beamwidth, and radiation pattern. Moreover, mutual coupling will also have an impact on the amplitude and phase of the transmitted signal and received signal by the array.

If the signal voltage received at each of the array's antenna is V_1, V_2, …, V_N in which $\widetilde{V}_1, \widetilde{V}_2, \ldots, \widetilde{V}_N$ are the voltages attributed to the mutual coupling effect, and Z_L is the load with a known impedance connected to each port. If Z_{ij} $(i = 1, 2, \ldots, N; j = 1, 2, \ldots, N)$ represents the mutual impedance caused by mutual coupling between the ith element and the jth element, and Z_{ii} is the impedance of the ith antenna element. The array can then be represented by the matrix

$$\begin{bmatrix} V_1 \\ V_2 \\ \vdots \\ V_N \end{bmatrix} = \begin{bmatrix} 1+\frac{Z_{11}}{Z_L} & \frac{Z_{12}}{Z_L} & \cdots & \frac{Z_{1N}}{Z_L} \\ \frac{Z_{21}}{Z_L} & 1+\frac{Z_{22}}{Z_L} & \cdots & \frac{Z_{2N}}{Z_L} \\ \vdots & \vdots & \ddots & \vdots \\ \frac{Z_{N1}}{Z_L} & \frac{Z_{N2}}{Z_L} & \cdots & 1+\frac{Z_{NN}}{Z_L} \end{bmatrix} \begin{bmatrix} \widetilde{V}_1 \\ \widetilde{V}_2 \\ \vdots \\ \widetilde{V}_N \end{bmatrix}$$

This matrix is represented hereon as

$$V = Z_o\widetilde{V}$$

where V is the signal voltage vector received at the array element with no coupling effect, $\widetilde{V}$ is the resulting output voltage vector at the array terminal, and Z_o is the normalized impedance matrix. If Z_o is known, the mutual coupling matrix C_o can be determined, and $C_o = Z_o^{-1}$. In our case the array element will use the voltage vector V_k of equal amplitude and equal phase difference as excitation, the specific expression of V_k is given by

$$V_k = \begin{bmatrix} 1 \\ e^{\frac{j2\pi d}{\lambda}\cos(\varphi)} \\ \vdots \\ e^{\frac{j2\pi(N-1)d}{\lambda}\cos(\varphi)} \end{bmatrix}$$

If the mutual coupling is not considered, the pattern of the N-element array can be expressed as [22]

$$f(\theta,\phi) = V_k^H A(\theta,\phi) F_k(\theta)$$

where $F_k(\theta)$ is the array element pattern, and $A(\theta,\phi)$ is the array manifold given by

$$A(\theta,\phi) = \begin{bmatrix} 1 \\ e^{\frac{j2\pi d}{\lambda}\cos(\theta)\cos(\varphi)} \\ \vdots \\ e^{\frac{j2\pi(N-1)d}{\lambda}\cos(\theta)\cos(\varphi)} \end{bmatrix}$$

If the mutual coupling effect is considered, the actual excitation

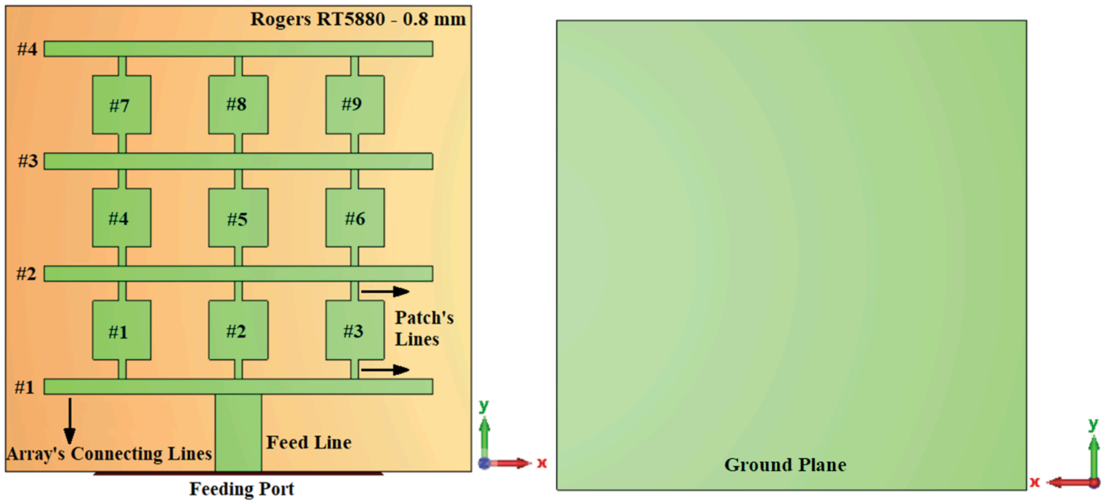

Fig. 2. Proposed antenna array #1 referred to here as the basic antenna array.

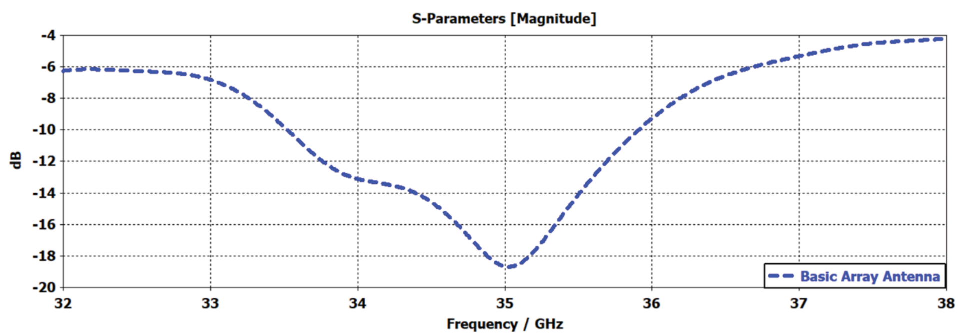

Fig. 3. Reflection coefficient response of the proposed array antenna #1.

voltage vector of the array element is

$$\widetilde{V}_k = C_o V_k$$

Therefore, the array's radiation pattern under the mutual coupling effect can be given as

$$\widetilde{f}(\theta, \phi) = V_k^H C_o^H A(\theta, \phi) F_k(\theta)$$

Due to the inverse relationship between the mutual coupling impedance and the element spacing, when the element spacing is small, the mutual coupling effect between the elements is strong, and the mutual coupling impedance is large. A detailed theoretical study on the influence of mutual coupling on the array's parameters is given in [22].

3. Design of the proposed antenna array

The initial antenna array proposed here will henceforth be referred to as the basic antenna array, which is shown in Fig. 2. Each array row accommodates three patch elements. The radiating elements are interconnected to each other, as shown in Fig. 2, where each row is interleaved with a horizontal microstrip-line whose ends are left open-circuited. The proposed structure mitigated unwanted electromagnetic interactions between the radiating elements that can undermine the radiation characteristics of arrays. Unlike in conventional arrays, the proposed structure is excited using a single feedline. The space between the radiating elements is designed such that there is phase coherency at the input of the radiators to mitigate undesirable sidelobes and ensure effective beam-steering is achieved over a wide angle. The patches are designed using established theory. The array is constructed from a matrix of 3 × 3 square patches on 0.8 mm thick Rogers RT5880 substrate

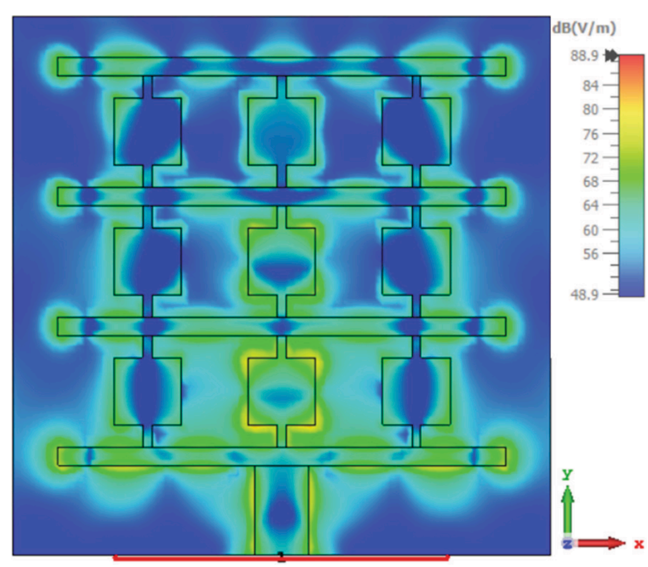

Fig. 4. Surface current density distribution over the proposed array at its resonance frequency of 35 GHz.

with dielectric constant of 2.2 and loss tangent of 0.0009. The dimensions of the array structure were optimized using CST Microwave Studio, which is a 3D full-wave solver based on the finite element method (FEM). The dimension of each patch is $3 \times 3\ \mathrm{mm}^2$ and the row of patches are separated by 3 mm. The length and width of (i) the

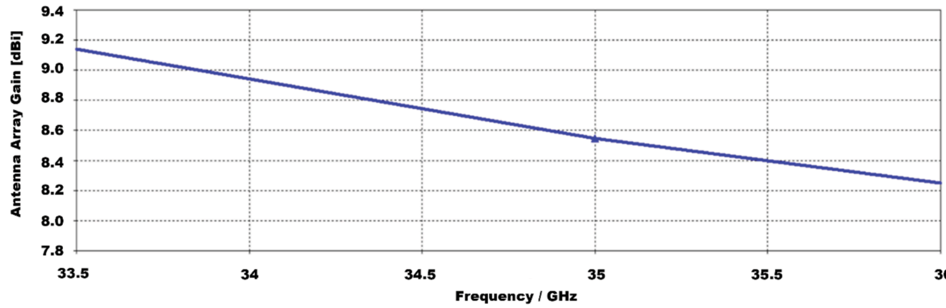

(a) Gain of the proposed basic antenna array

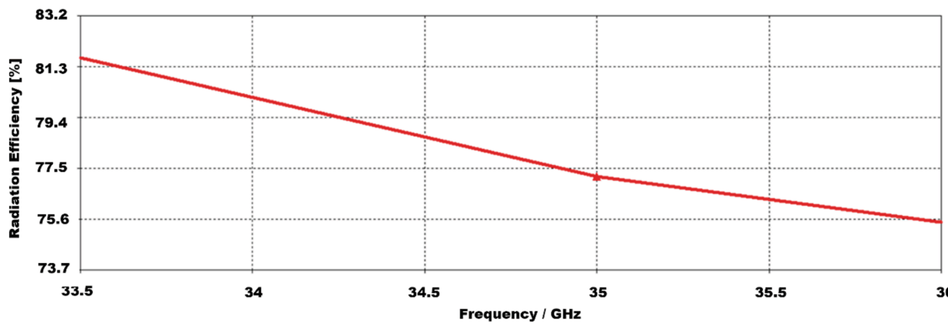

(b) Radiation efficiency of the proposed basic antenna array

Fig. 5. Simulated gain and radiation efficiency of the proposed antenna array over 33.5 GHz to 35.9 GHz.

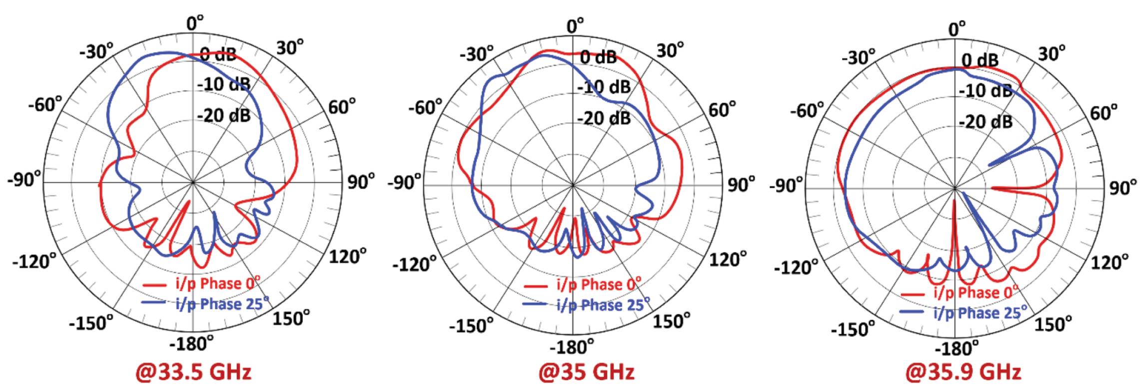

(a) *yz*-plane

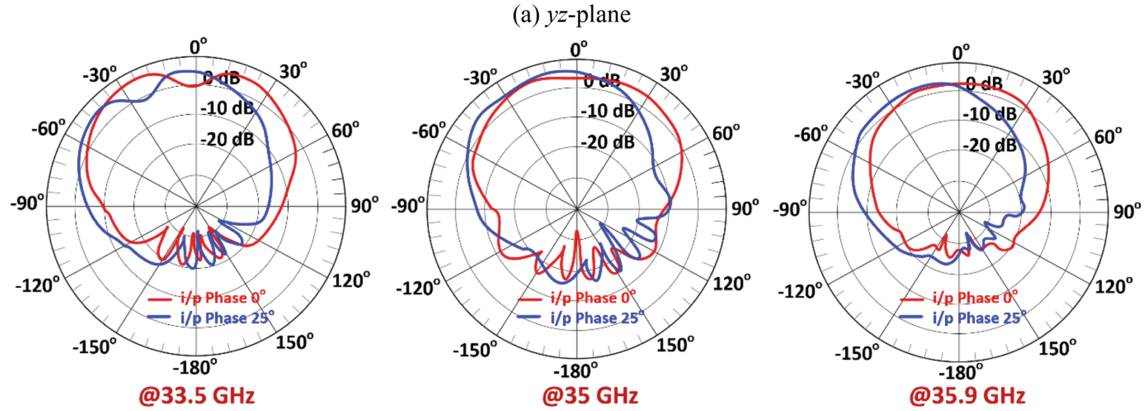

(b) *xz*-plane

Fig. 6. Simulated radiation patterns of the proposed antenna array #1 in the *yz*-plane and *xz*-plane at 33.5 GHz, 35.0 GHz, and 35.9 GHz for excitation phase angle of 0 degree and 25 degrees.

microstrip feedline are 4 mm & 2.4 mm, respectively; (ii) the horizontal connecting lines are 20 mm & 0.8 mm, respectively; and (iii) the vertical lines at each radiating element are 1 mm & 0.4 mm, respectively. The overall dimensions of the array are 24 × 24 × 0.8 mm^3. The back side of array board is a ground-plane. Unlike prior techniques the proposed technique avoids the use of decoupling structures and multiple feeding

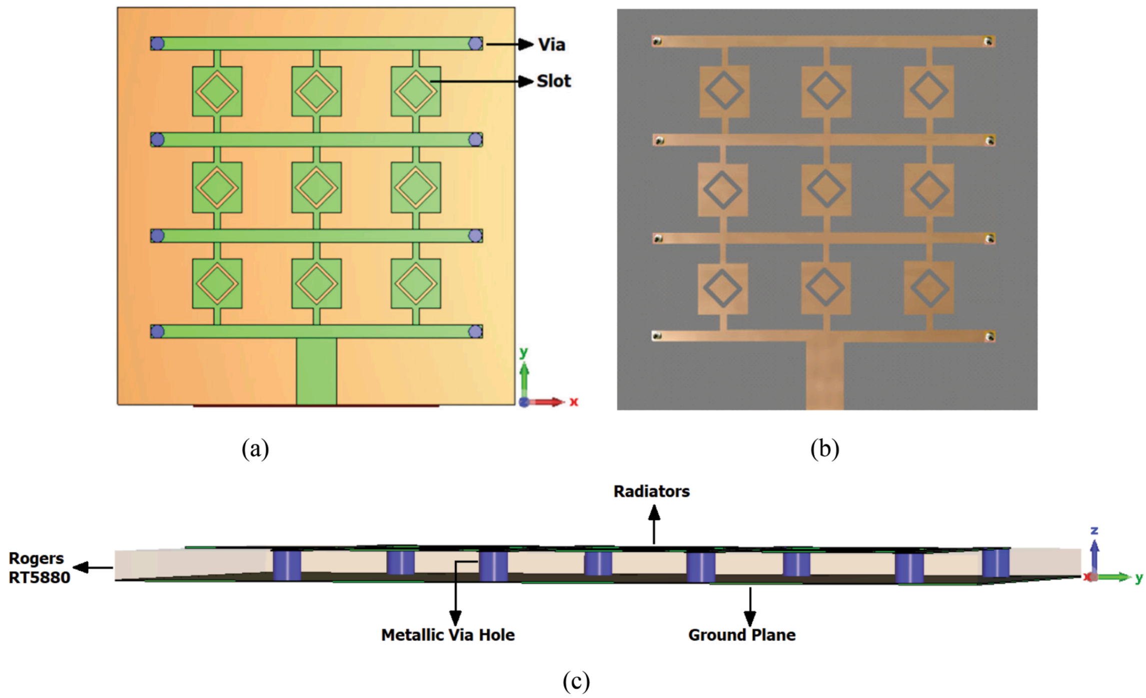

Fig. 7. Proposed antenna array including metamaterial inspired modifications, (a) modelled top-view layout, (b) fabricated array, and (c) modelled side-view.

ports.

The simulated reflection coefficient response of the proposed basic antenna array is shown in Fig. 3. The proposed antenna array was modelled and simulated using CST Microwave Studio. The array operates over a frequency range of 33.5 GHz to 35.9 GHz for $S_{11} \leq$ -10 dB, which corresponds to a fractional bandwidth of 6.91 %. The array resonates at 35 GHz with an impedance matching performance of −18.6 dB. Fig. 4 shows the surface current density distribution over the array at the resonant frequency of 35 GHz. As expected, the concentration of the current distribution is strongest on the array structure nearest the feedline. In fact, the radiating element immediately next to the feedline has the strongest accumulation of current over it, and therefore is the dominant radiator in the array.

The simulated gain and radiation efficiency of the proposed basic antenna array across 33.5 GHz to 36 GHz is shown in Fig. 5. The average gain and efficiency across the given frequency span are 8.7 dBi and 78.6 %, respectively. The maximum gain and efficiency are obtained at 33.5 GHz, which are 9.15 dBi and 81.6 %, respectively. These results show an identical correlation between the gain and efficiency performance of the array. The simulated radiation patterns of the array in the *yz*- and *xz*-planes at the spot frequencies of 33.5 GHz, 35 GHz, and 35.9 GHz are shown in Fig. 6. In the *yz*-plane the array radiates energy in the broadside with a 3 dB beamwidth of 60 degrees at 33.5 GHz and 35 GHz. However, at 35.9 GHz it radiates over beamwidth angle of 150 degrees. In the *xz*-plane at 33.5 GHz it radiates bidirectionally with a 3 dB beamwidth of 50 degrees, however at 35 GHz and 35.9 GHz it radiates unidirectionally with beamwidths of 120 degrees and 75 degrees, respectively.

Fig. 6 shows how the beam steering is accomplished by changing the phase of the excitation signal. Although the beamwidth is relatively large compared to conventional arrays however beam steering observed is distinct. In Fig. 6 the phase of the excitation signal is changed from 0 degree to 25 degrees and there is a corresponding change in the direction of the main beam as predicted by the general array theory in Section III. This feasibility study confirms proof-of-concept by the proposed technique.

It is now shown how the array's performance can be improved without affecting its dimensions. This is achieved by employing innovative approach that is metamaterial inspired. The top side of the array is connected to its ground-plane through by short-circuiting the open-ends of the horizontal lines partitioning the rows of radiating elements using metal via-pins of 0.8 mm diameter, as shown in Fig. 7. This procedure suppresses undesired surface coupling between the radiating elements. In addition, each patch is loaded with a rhombus shaped slot with length and width of each side of 1.5 mm and 0.3 mm, respectively, that enlarges the effective aperture of the radiators. The slots in

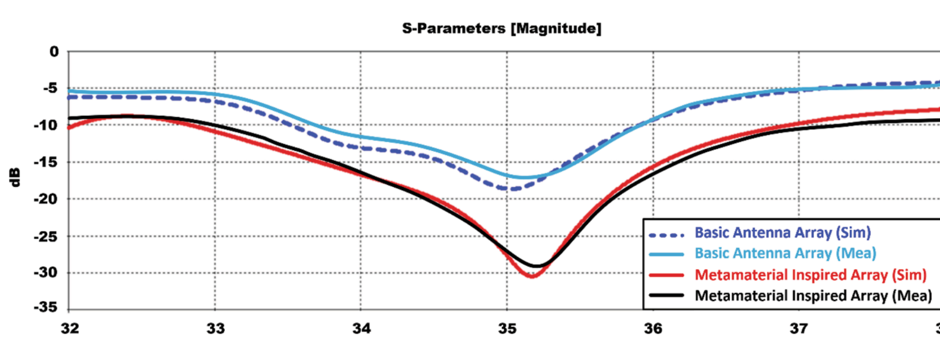

Fig. 8. Simulated and measured reflection coefficient response of the proposed basic array and the proposed metamaterial inspired antenna array.

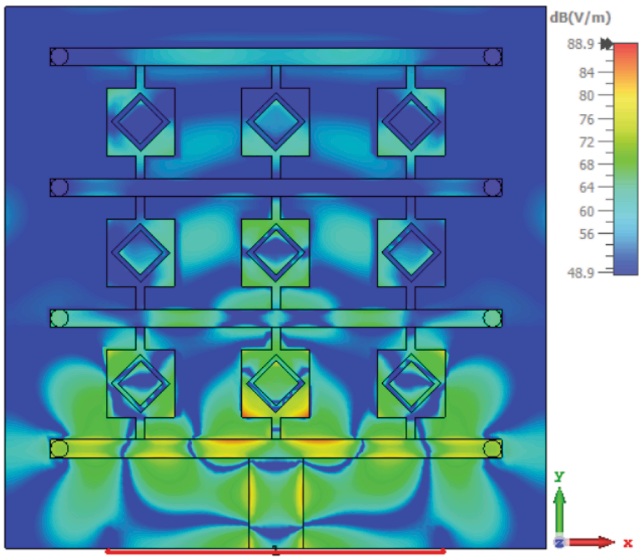

Fig. 9. Surface current density distribution over the proposed metamaterial inspired antenna array at its resonance frequency of 35.2 GHz.

combination with the short-circuited lines created composite right/left-handed or metamaterial structure as explained in [23].

The measured and simulated reflection coefficient response of the proposed basic antenna array and the modified array are shown in Fig. 8. There is excellent agreement between the CST Microwave Studio simulated response and the measured results. Compared to the proposed basic array, the measured results show that the proposed metamaterial inspired array exhibits impedance bandwidth extension of 4.2 GHz from 32.8 GHz to 37.0 GHz for $S_{11} \leq$ -10 dB, which corresponds to a fractional bandwidth of 12.03 %. At the measured resonance frequency of 35.2 GHz, the impedance match of the metamaterial inspired array is −30.5 dB, which an improvement of 11.5 dB. This reveals the effectiveness of the proposed design technique. The surface current density distribution at the resonant frequency of 35.02 GHz is shown in Fig. 9. Although the surface current is concentrated in the region of the array structure connected to the feedline however it can be discerned by comparing with Fig. 4 that the shorted circuited horizonal lines have significantly reduced surface currents.

The simulated and measured gain and efficiency of the proposed metamaterial inspired antenna array is shown in Fig. 10. There is excellent correlation between the measured and simulation results. The gain and radiation efficiency decrease in an almost linear fashion from 33 GHz to 37 GHz. At the measured gain is 13.45 dBi and at 37 GHz it reduces to 8.3 dBi. At the array's resonance frequency of 35.2 GHz the gain and efficiency are 10.2 dBi and 82.41 %, respectively. Compared to the proposed basic antenna array the metamaterial inspired array provides improvement in gain and efficiency of 1.6 dBi and 5.64 %, respectively.

The simulated and measured radiation patterns of the metamaterial inspired array in the *yz*- and *xz*-planes at 33.0 GHz, 35.2 GHz, and 37.0 GHz are shown in Fig. 11. The array radiates in energy in unidirectionally at all three spot frequencies. The radiation in the *yz*-plane is focused and more symmetrical at the array's resonance frequency of 35.2 GHz. The measured 3 dB beamwidth at 33 GHz is 32 degrees, at 35.2 GHz is 29 degrees, and at 37 GHz is 50 degrees. Similarly, in the *xz*-plane the array radiates unidirectionally. In the *xz*-plane the measured 3 dB beamwidth at 33 GHz is 40 degrees, at 35.2 GHz is 37 degrees, and at 37 GHz is 44 degrees. Fig. 6 also shows how the radiation beam is steered with change in the excitation signal from 0 degree to 25 degrees. This feasibility study confirms proof-of-concept by the proposed technique.

The above results demonstrate that the proposed technique can be implemented on a tightly packed antenna array designed to operate in the millimeter band of the electromagnetic spectrum. Moreover, the radiation characteristics of the array is stable over its operating frequency range. These properties make the antenna suitable for various millimeter-wave applications including 5G and future communications and radar systems.

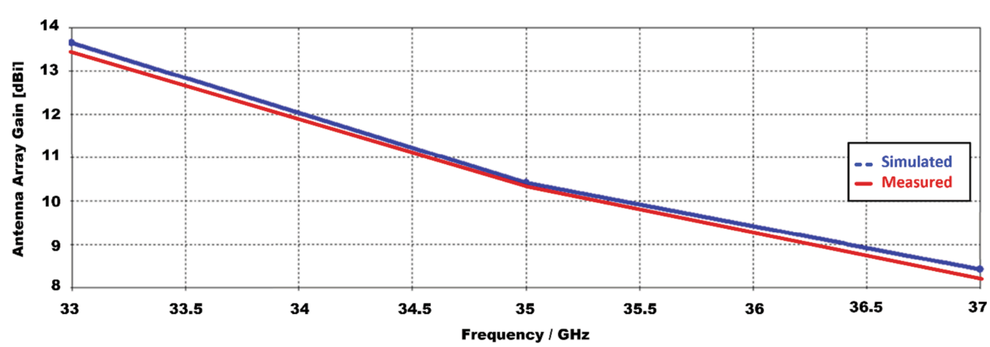

(a) Antenna realized gain

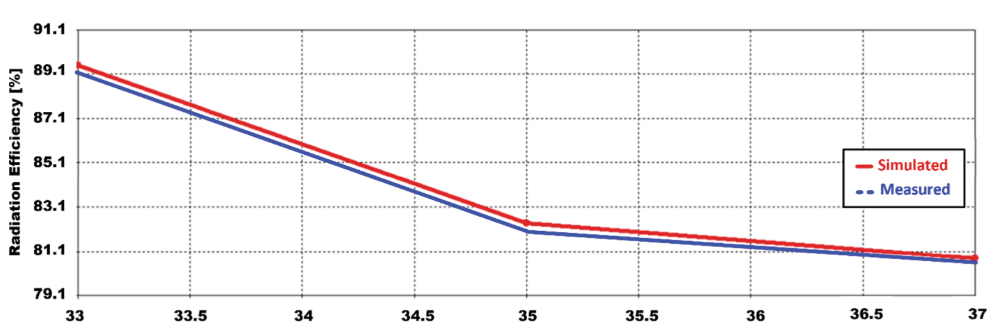

(b) Radiation efficiency

Fig. 10. Simulated and measured gain and radiation efficiency of the proposed metamaterial inspired antenna array.

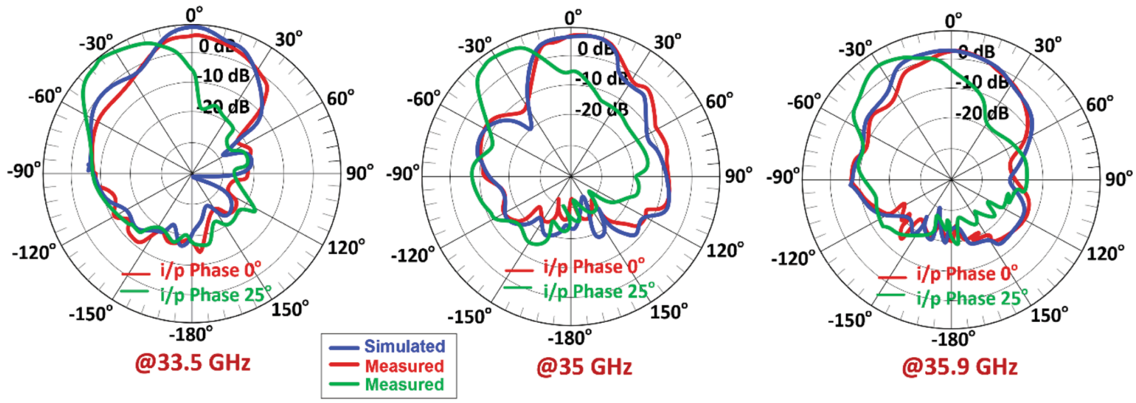

(a) *yz*-plane

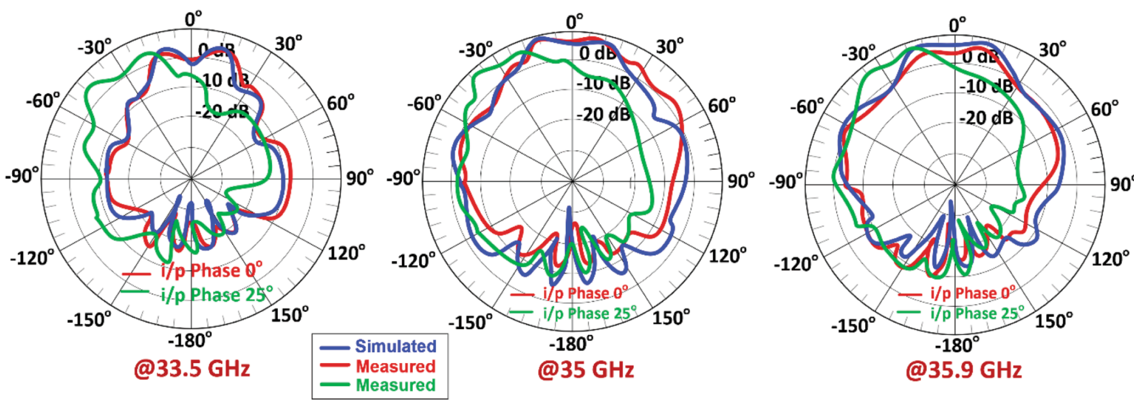

(b) *xz*-plane

Fig. 11. Simulated and measured radiation patterns in the *yz*-plane and *xz*-plane at 33.0 GHz, 35.2 GHz, and 37.0 GHz for excitation phase angle of 0 degree and 25 degrees.

Table 1
Comparison with prior works.

Ref.	Technique	Dimensions (λ_0^2)	Frequency band (GHz)	Edge-to-edge space (λ_0)	No of ports	Port isolation (dB)	Max. gain (dBi)	Max. efficiency (%)	Design complexity
[24]	Metamaterial	4.42 × 1.95	24.0 – 29.9	0.36	2	24	13.4	98	Moderate
[25]	Via	1.98 × 5.82	25.2 – 27.1	0.11	2	30	6.6	–	High
[26]	Metasurface	–	24.2 – 27.8 36.9 – 42.8	–	2	24	11	83	Moderate
[27]	Slot	3.89 × 1.47	22.5 – 50.0	5.25	2	20	15	84	Moderate
[28]	Dielectric resonator	4.82 × 2.10	29.7 – 31.5	0.28	2	25	7	80	High
[29]	EBG & DGS	3.87 × 3.6	27.5 – 28.35	0.54	2	32.7	9	81.9	High
This work	**Metamaterial inspired**	**2.64 × 2.64**	**33.0 – 37.0**	**0.32**	**1**	**N/A**	**13.6**	**89.54**	**Low**

4. State-of-the-Art Comparison

The characteristics of the proposed metamaterial inspired antenna array is compared in Table 1 with other recently reported mutual coupling reduction techniques. As is evident in Table 1, one of the main advantages of the proposed technique is that the array is excited using a single port and therefore port isolation is not an issue. Moreover, compared to the cited prior techniques in Table 1 the dimensions of the proposed antenna array are much smaller because the radiating elements can be squeezed closer to each other, and the array is less complex to fabricate.

5. Conclusion

Verified here is the design of a novel millimeter-wave antenna array with advantage of not requiring a separate decoupling structure, can be applied in a densely packed array, and is excited using a single feedline. The metamaterial inspired array comprises 3 × 3 matrix of interconnected square patches that are embedded with a rhombus shaped slot to enlarge the effective aperture of the antenna without comprising the antenna size. The rows of radiating elements are partitioned from each other with horizontal short-circuited microstrip-line. This technique effectively stops surface waves interacting with the radiating elements. The space between the radiator elements and interconnected feedlines is made to ensure the phase coherency at the radiators. The radiation patterns of the proposed array are stable over its operating band. The array can be employed in various millimeter wave devices and systems including 5G and 6G communications, automotive and radar systems.

Declaration of Competing Interest

The authors declare that they have no known competing financial interests or personal relationships that could have appeared to influence the work reported in this paper.

Data availability

No data was used for the research described in the article.

Acknowledgment

This work was funded by the Deanship of Scientific Research at Jouf University under Grant Number (DSR2022-RG-0110).

References

[1] ITU's World Radio Conference 2019 (WRC-19).
[2] Andrews JG, Buzzi S, Choi W, Hanly SV, Lozano A, Soong ACK, et al. What will 5G be? IEEE J Sel Areas Commun Jun. 2014;32(6):1065–82.
[3] Attiah ML, Isa A, Zakaria Z, Abdulhameed M, Mohsen MK, Ali I. A survey of mmWave user association mechanisms and spectrum sharing approaches: An overview, open issues and challenges, future research trends. Wireless Netw 2020;26(4):2487–514.
[4] Althuwayb AA, et al. 3-D-printed dielectric resonator antenna arrays based on standing-wave feeding approach. IEEE Antennas Wirel Propag Lett Oct. 2019;18(10):2180–3.
[5] Jamshed MA, et al. Dual band and dual diversity four-element MIMO dipole for 5G handsets. Sensors 2021;21:767.
[6] Gaya A, et al. Circular patch fed rectangular dielectric resonator antenna with high gain and high efficiency for millimeter wave 5G small cell applications. Sensors 2021;21:2694.
[7] Rappaport TS, Xing Y, MacCartney GR, Molisch AF, Mellios E, Zhang J. Overview of millimeter wave communications for fifth generation (5G) wireless networks—With a focus on propagation models. IEEE Trans Antennas Propag Dec. 2017;65(12):6213–30.
[8] Zhang Y, Deng J-Y, Li M-J, Sun D, Guo L-X. A MIMO dielectric resonator antenna with improved isolation for 5G mm-wave applications. IEEE Antennas Wireless Propag Lett Apr. 2019;18(4):747–51.
[9] Mchbal A, Amar Touhami N, Elftouh H, Dkiouak A. Mutual coupling reduction using a protruded ground branch structure in a compact UWB owl-shaped MIMO antenna. Int J Antennas Propag Sep. 2018, 2018,:1–10.
[10] Wang F, Duan Z, Wang X, Zhou Q, Gong Y. High isolation millimeter-wave wideband MIMO antenna for 5G communication. Int J Antennas Propag May 2019;2019:1–12.
[11] Singh H, Sneha HL, Jha RM. Mutual coupling in phased arrays: a review. International Journal of Antennas and Propagation 2013:1–23.
[12] See CH, et al. A comprehensive survey on various decoupling mechanisms with focus on metamaterial and metasurface principles applicable to SAR and MIMO antenna systems. IEEE Access 2020;8:192965–3004.
[13] Nadeem I, Choi D. Study on mutual coupling reduction technique for MIMO antennas. IEEE Access 2019;7:563–86.
[14] Karimian R, Kesavan A, Nedil M, Denidni TA. Low-mutual coupling 60-GHz MIMO antenna system with frequency selective surface wall. IEEE Antennas Wireless Propag Lett 2017;16:373–6.
[15] Lin FH, Chen ZN. Low-profile wideband metasurface antennas using characteristic mode analysis. IEEE Trans Antennas Propag Apr. 2017;65(4):1706–13.
[16] Li T, Chen ZN. A dual-band metasurface antenna using characteristic mode analysis. IEEE Trans Antennas Propag Oct. 2018;66(10):5620–4.
[17] Assimonis SD, Yioultsis TV, Antonopoulos CS. Design and optimization of uniplanar EBG structures for low profile antenna applications and mutual coupling reduction. IEEE Trans Antennas Propag Oct. 2012;60(10):4944–9.
[18] Abdalrazik A, El-Hameed ASA, Abdel-Rahman AB. A three port MIMO dielectric resonator antenna using decoupled modes. IEEE Antennas Wireless Propag Lett 2017;16:3104–7.
[19] Lee Y, Ga D, Choi J. Design of a MIMO antenna with improved isolation using MNG metamaterial. Int J Antennas Propag Jul. 2012;2012:1–7.
[20] Q.-L. Zhang, Y.-T. Jin, J.-Q. Feng, X. Lv, and L.-M. Si, "Mutual coupling reduction of microstrip antenna array using metamaterial absorber," IEEE MTT-S Int. Microw. Symp. Dig. Ser. Adv. Mater. Processes RF THz Appl. (IMWS-AMP), Jul. 2015, pp. 1–3.
[21] Farahani M, Pourahmadazar J, Akbari M, Nedil M, Sebak AR, Denidni TA. Mutual coupling reduction in millimeter-wave MIMO antenna array using a metamaterial polarization-rotator wall. IEEE Antennas Wireless Propag Lett 2017;16:2324–7.
[22] Xiong Y, Xie W. Adaptive mutual coupling compensation method for airborne STAP radar with end-fire array. IEEE Trans Aerosp Electron Syst 2022;58(2):1283–98.
[23] Alibakhshikenari M, Naser-Moghadasi M, Sadeghzadeh RA, Virdee BS, Limiti E. Printed planar antenna designs based on metamaterial unit-cells for broadband wireless communication systems. Trends in Research on Microstrip Antennas, Chapter 2017;2. https://doi.org/10.5772/intechopen.68600.
[24] Al-Bawri SS, Islam MT, Shabbir T, Muhammad G, Islam MS, Wong HY. Hexagonal Shaped Near Zero Index (NZI) Metamaterial Based MIMO Antenna for Millimeter-Wave Application. IEEE Access 2020;8:181003–13.
[25] Pan YM, Qin X, Sun YX, Zheng SY. A simple decoupling method for 5G millimeter-wave MIMO dielectric resonator antennas. IEEE Trans Antennas Propag Apr. 2019;67(4):2224–34.
[26] B. Feng, X. He, J.-C. Cheng, and C.-Y.-D. Sim, "Dual-wideband dual polarized metasurface antenna array for the 5G millimeter wave communications based on characteristic mode theory," IEEE Access, vol. 8, pp. 21589–21601, 2020; R. Chandel, A. K. Gautam, and K. Rambabu, "Tapered fed compact UWB MIMO-diversity antenna with dual band-notched characteristics," IEEE Trans. Antennas Propag., vol. 66, no. 4, pp. 1677–1684, Apr. 2018.
[27] A. A. R. Saad and H. A. Mohamed, "Printed millimeter-wave MIMO-based slot antenna arrays for 5G networks," AEU-Int. J. Electron. Commun., vol. 99, pp. 59–69, Feb. 2019; M. S. Sharawi, S. K. Podilchak, M. T. Hussain, and Y. M. M. Antar, "Dielectric resonator based MIMO antenna system enabling millimetre wave mobile devices," IET Microw., Antennas Propag., vol. 11, no. 2, pp. 287–293, Jan. 2017.
[28] Jaglan N, Gupta SD, Thakur E, Kumar D, Kanaujia BK, Srivastava S. Triple band notched mushroom and uniplanar EBG structures based UWB MIMO/diversity antenna with enhanced wide band isolation. AEU-Int J Electron Commun Jun. 2018;90:36–44.
[29] Dey S, Dey S, Koul SK. Isolation Improvement of MIMO Antenna Using Novel EBG and Hair-Pin Shaped DGS at 5G Millimeter Wave Band. IEEE Access 2021:162820–34.

Ayman A. Althuwayb received the B.Sc. degree (Hons.) in electrical engineering (electronics and communications) from Jouf University, Saudi Arabia, the M. Sc. Degree in electrical engineering from California State University, Fullerton, CA, USA, in 2015, and the Ph.D. degree in electrical engineering from Southern Methodist University, Dallas, TX, USA, in 2018. He is currently an Assistant Professor with the department of electrical engineering at Jouf University, Kingdom of Saudi Arabia. His current research interests include antenna design and propagation, microwaves and millimeter-waves, wireless power transfer, ultra-wideband and multiband antenna, filters and others.

Mohammad Alibakhshikenari was born in Mazandaran, Iran, in February 1988. He received the Ph.D. degree (Hons.) with European Label in electronics engineering from the University of Rome "Tor Vergata'', Italy, in February 2020. He was a Ph.D. Visiting Researcher at the Chalmers University of Technology, Sweden, in 2018. His training during the Ph.D. included a research stage in the Swedish company Gap Waves AB. He is currently with the Department of Signal Theory and Communications, Universidad Carlos III de Madrid (uc3m), Spain, as the Principal Investigator of the CONEX-Plus Talent Training Program and Marie Sklodowska-Curie Actions. He was also a Lecturer of the electromagnetic fields and electromagnetic laboratory with the Department of Signal Theory and Communications for academic year 2021–2022 and he received the "Teaching Excellent Acknowledgement'' Certificate for the course of electromagnetic fields from Vice-Rector of studies of uc3m. His research interests include electromagnetic systems, antennas and wave-propagations, metamaterials and metasurfaces, synthetic aperture radars (SAR), multiple input multiple output (MIMO) systems, RFID tag antennas, substrate integrated waveguides (SIWs), impedance matching circuits, microwave components, millimeter-waves and terahertz integrated circuits, gap waveguide technology, beamforming matrix, and reconfigurable intelligent surfaces (RIS). He was a recipient of the three years research grant funded by Universidad Carlos III de Madrid and the European Union's Horizon 2020 Research and Innovation Program under the Marie Sklodowska-Curie Grant started in July 2021, the two years research grant funded by the University of Rome "Tor Vergata'' started in November 2019, the three years Ph.D. Scholarship funded by the University of Rome "Tor Vergata'' started in November 2016, and the two Young Engineer Awards of the 47th and 48th European Microwave Conference were held in Nuremberg, Germany, in 2017, and in Madrid, Spain, in 2018, respectively. His research article entitled "High-Gain Metasurface in Polyimide On-Chip Antenna Based on CRLH-TL for Sub Terahertz Integrated Circuits'' published in Scientific Reports was awarded as the Best Month Paper at the University of Bradford, U.K., in April 2020. He is serving as an Associate Editor for (i) Radio Science, (ii) IET Journal of Engineering, and (iii) International Journal of Antennas and Propagation. He also acts as a referee in several highly reputed journals and international conferences.

Bal S. Virdee graduated with a B.Sc. (Eng.) from the University of Leeds, U.K., and Ph.D. degree from the University of London, U.K. Since graduation he has worked in industry for various high-tech companies including Philips, as a research and development engineer, and at Teledyne Defence & Space as a future products developer in RF/microwave communications. He has taught in several academic institutions in the U.K. He is currently a senior professor of communications technology and director of center for communications technology at the school of computing and digital media, London Metropolitan University. He has supervised and examined numerous PhD students and has published extensively research papers at international conferences and peer-reviewed journals. His research, in collaboration with industry and academia, is in next generation wireless communications systems. He is Chair and Executive Member of the Institution of Engineering and Technology's (IET) technical and professional network committee on RF/microwave-technology. He is a charted engineer (CEng), Fellow of the IET and Senior Member of IEEE.

Harry Benetatos is a senior lecturer in the School of Computing and Digital Media and also acts as course leader for Computer Networking and Cyber Security MSc. Harry holds an MSc in Internet Technology and a BSc (Hons) in Electronic and Communications Engineering. He is a Cisco instructor for CCNA, CCNP, Fundamentals of Network Security, IT Essentials I and II. His areas of expertise are in peer-to-peer networking, distance learning, IT security, and computer networking.

Nasr Rashid was born in Egypt, in 1973. He received the B.Sc. (with highest honors), M.Sc, and PhD in Electronics and Communication Engineering from Al-Azhar University, Cairo, Egypt in 1996, 2004, and 2009 respectively. He is currently an Assistant Professor in the Department of Electrical Engineering, College of Engineering, Jouf University, Sakaka, Saudi Arabia. His current research interests are in wireless communications, antennas and wave-propagations, control engineering, and signal processing.

Khaled Kaaniche was born in Tunisia in 1976. He received the BSc degree in Electrical Engineering from University of Sfax, Tunisia in 2000. In 2001, he received MSc degree in Control from INSA Lyon, France and in 2005 the Ph.D. degree in Control from UPJV France. He joined the University of Sousse, Tunisia in 2006 as an Assistant Professor in the College of Engineering. Between 2010 and 2014 he was the head of the Computer Engineering Department. His main areas of research interest are Visual Servo, Robotics, Optimization and Computer Vision. He is currently an assistant professor in the Electrical Engineering Department at Jouf University, Saudi Arabia.

Ahmed Ben Atitallah is currently an Associate Professor in Electronics at College of Engineering, Jouf University, Kingdom of Saudi Arabia. He received his PhD degree in Electronics from the University of Bordeaux1 in 2007, France and the diploma of engineer and MS degree in Electronics from the University of Sfax in 2002 and 2003, respectively, Tunisia. From 2008 to 2018, he held the position of assistant professor then associate professor in Electronics at the University of Sfax, Tunisia. His main research activities are focused on image and video processing, Algorithm-Architecture Matching, Hardware/Software Codesign, SoC/SoPC architecture, Design space exploration, Parallel architecture, Reconfigurable computing.

Osama I. Elhamrawy was born in Egypt, in 1976. He received the B.S., M.S, and PhD in Electronics and Communication Engineering from Al-Azhar University, Cairo, Egypt in 1999, 2006, and 2011 respectively. He is currently an Assistant Professor in the Department of Electrical Engineering, College of Engineering, Jouf University, Sakaka, Saudi Arabia. His current research interests are in Electronics, Multilevel Inverters, and Wireless Communications.